Automated measurement of concrete spalling through reinforcement detection

Stephanie German Paal*

School of Architecture, Civil and Environmental Engineering, Ecole Polytechnique Fédérale de Lausanne, Lausanne, Switzerland

Ioannis Brilakis

Department of Engineering, University of Cambridge, Cambridge, UK

&

Reginald DesRoches

School of Civil Engineering, Georgia Institute of Technology, Atlanta, GA, USA

Abstract: *In emergency scenarios, immediate reconnaissance efforts are necessary. These efforts often take months to complete in full. While underway, building occupants are unable to return to their homes/businesses, and thus, the impact on the society of the disaster-stricken region is increased. In order to mitigate the impact, researchers have focused on creating a more efficient means of assessing the condition of buildings in the post-disaster state. In this paper, a machine vision-based methodology for real-time post-earthquake safety assessment is presented. A novel method of retrieving spalled properties on reinforced concrete (RC) columns in RC frame buildings using image data is presented. In this method, the spalled region is detected using a local entropy-based approach. Following this, the depth properties are retrieved using contextual information pertaining to the amount and type of reinforcement which is exposed. The method is validated using a dataset of damaged RC column images.*

1 INTRODUCTION

Since the start of 2013, there have been over 1,700 earthquakes of magnitude 5.0 or higher worldwide (USGS, 2012). Moreover, earthquakes have been acknowledged as one of the most costly natural hazards faced in the United States, posing a major threat to at least 75 million Americans in 39 states (USGS, 2006). In order to mitigate the effects of such natural disasters, a more responsive government is necessary. The following four goals have been established by the United States Geological Society (USGS) in order to meet this need in the US (USFA, 1994): (1) enhanced observations; (2) fundamental understanding of hazards and impacts; (3) improved assessment products and services; and (4) effective situational awareness. Several research efforts have been initiated by the USGS in the direction of enhanced observations (1), improved fundamental understanding of the hazards and impacts (2) as well as enhanced situational awareness (4) byway of programs such as the Earthquake Early Warning (EEW) System, ground motion studies, hazard mapping projects, etc. (McEntire and Cope, 2004). The third goal concerning improved assessment products and services remains untouched by the USGS, and thus, post-earthquake response procedures still lack robustness and efficiency. Guidelines for structural evaluations after an earthquake event have been previously established by government agencies such as the Applied Technology Council (ATC) and the Federal Emergency Management Agency (FEMA). These evaluations are carried out by a team of specialists including a certified structures specialist who makes the assessment regarding the safety of the building based on experience, knowledge and visual observation of the damage inflicted on the load-bearing members of the structure. The large inventory of damaged buildings characteristic in the aftermath of a significant natural disaster such as an earthquake far exceeds the capacity of these search and rescue teams. This paper focuses on enhancing the post-earthquake safety assessment procedures in line with the established goals of the USFS.

In order to overcome the inherent limitations of the current practices in post-earthquake safety and structural evaluations, there have been various efforts towards automating these procedures. These efforts include those in the research fields of Structural Health Monitoring (SHM), Remote Sensing and Computer Vision primarily. They focus on using visual date retrieved from building sites or satellites and evaluating the data with or without the aid of other documents such as building drawings and measurements. The results of these various efforts range in the amount of detail which is provided, from the city- or building-wide level (satellite imagery) to the specific damage on these specific elements (SHM and Machine Vision). These methods have been tested in a wide-range of structures such as concrete bridges, pipes, tunnels and buildings, and the results of these tests do verify the ability of their application for detecting damage in assessment-based practices. However, in order to

provide a rapid and reliable (quantitative) evaluation of the structural element which is indicative of the existing structural integrity of the member, there exists several gaps in the aforementioned research efforts which are to be addressed by this work. First, although some damage types have been explored to a substantial depth, critical types of damage which are indicative of the remaining structural integrity of a member have yet to be addressed. In addition, the detected damage has not been correlated with the surface (structural member) on which it exists. This prevents the quantification of the damage in a manner which is meaningful for the structural assessment of the member and the building as a whole. The main purpose of this research is to investigate the means to fill these gaps.

This paper presents a novel approach for retrieving key properties of spalled regions on reinforced concrete (RC) structural element surfaces. In this work, the extent (depth) of spalling is classified with respect to one of five categories: (1) no spalling; (2) spalling of concrete cover—no exposure of reinforcement; (3) spalling which exposes transverse reinforcement; (4) spalling which exposes longitudinal reinforcement; and (5) spalling of concrete which exposes both transverse and longitudinal reinforcement. The authors have previously published the results of work which made efforts to compress the classification of the depth of spalling into the following two categories: (1) spalling of cover with no exposure of reinforcement or just transverse reinforcement exposure (combines 2 and 3 of above), and (2) spalling with exposed longitudinal reinforcement and beyond (combines 4 and 5 of above). Thus, in further detail, this paper presents a novel approach for detecting transverse reinforcement and distinguishing it from longitudinal reinforcement. In addition, the algorithms for spalling detection and property retrieval presented herein are designed such that the absence of spalled regions on concrete surfaces can be sufficiently detected.

The approach was implemented in a Microsoft Visual .NET environment. A database of RC column surface images collected from buildings damaged in the 2010 earthquake in Haiti is used to test the approach's validity. The results from the approach are compared with those from manual surveys to determine the measurement error for each of the five categorizations of extent of spalling. According to the test results, it is found that the properties of the spalled region on structural elements can be correctly determined using the proposed method.

2 BACKGROUND

Currently, the procedures in post-earthquake assessment of practices are performed manually by a team of certified inspectors. These existing procedures in post-earthquake assessments are time-consuming, and with the imminent nature of the completion of these assessments in order to reduce the economic and societal impact associated with the downtime after an earthquake, this is a vital issue. In addition to being time-consuming, the subjective nature of evaluating building safety and structural integrity can lead to erroneous judgments. Thus, there is a need for improvement of the existing assessment procedures such that they are rapid (real-time) and more reliable.

Immediately after a disaster event, such as an earthquake, community response teams (most often trained by the local fire department) are first dispatched for a drive-through assessment to identify locations of heavy damage and high potential of trapped victims throughout the affected area (USFA, 1994; McEntire and Cope, 2004). The assessment is commonly interrupted by fires and other hazards causing immediate threat to lives. After initial assessments, due to the drastic effects in the aftermath of such disasters, local emergency response teams often call for backup from US&R task forces (or the equivalent government established response task force in other countries). These task forces follow standard operating procedures in conjunction with the community emergency response team, which may vary according to locality and situation. When a disaster such as an earthquake affects multiple structures, the prioritization of damaged buildings before any search and rescue operations commence is required. There are extensive risks for people entering these buildings damaged by an earthquake, and any further structural collapse (likely due to aftershocks) could quickly transform these task force members from emergency responders into additional victims. Therefore, it is essential to evaluate the level of safety associated with damaged buildings in post-earthquake scenarios prior to the entry of emergency search and rescue teams.

2.1 State of practice in post-earthquake assessment

In current practice, safety and structural evaluations of damaged buildings in a post-earthquake scenarios are carried out in

Table 1
ATC-20 stages of building evaluation (ATC, 1995)

Technique	Required Personnel	Goal	Example Time per Building
Rapid Evaluation	• Qualified building inspectors • Civil/structural engineers • Architects • Other individuals deemed qualified by local jurisdiction	• Rapid assessment of safety • Used to quickly post obviously unsafe and safe structures, and to identify buildings requiring Detailed Evaluation	10-20 minutes
Detailed Evaluation	• Structural engineers*	• Careful visual evaluation of damaged buildings and questionable situations • Used to identify buildings requiring an Engineering evaluation	1-4 hours
Engineering Evaluation	• Structural engineering consultant	• Detailed engineering investigation of damaged buildings, involving use of construction drawings, damage data and new structural calculations	1-7 days or more

*Geotechnical specialists required for assessment of geotechnical hazards

two phases: (1) safety evaluation prior to entry of the search and rescue teams; and (2) structural evaluations prior to re-entry by the building occupants and owners. These procedures are designated to be performed by a team of various specialists (e.g., a technical search specialist, a structures specialist, a medical specialist, a Haz-Mat specialist, rescue specialists, etc.) (FEMA, 2006). Due to the conglomerate nature of these teams, collaboration-related problems including lack of coordination, information sharing, trust and communication, between the various specialists involved in the disaster relief efforts have been identified (Kostoulas et al., 2006). The operations are organized into several phases depending on the amount and type of information which should be retrieved and that which has already been retrieved in previous phases. In each of the assessment phases, the information is retrieved manually by the designated structural specialists on the triage team. As these phases progress, the amount and type of information retrieved becomes increasingly complex and thus, time-intensive (Table 1). During the assessment procedures the structural specialists are expected to be the most prepared personnel to deal with all aspects of the built environment in urban areas (Aldunate et al., 2006). The involved structural specialists are responsible for identifying potential structural hazards and monitoring the structure for condition changes during the rescue and recovery operations (FEMA, 2008). It is suggested that two or more specialists work together, but that is impractical in emergency response to large disasters (ATC, 1995; FEMA, 2009). There are typically not enough qualified structural specialists for allocation to the individual community emergency response teams. In addition, those that can participate must be licensed professional engineers with a minimum of five years of experience (FEMA, 2008).

2.2 Recent research efforts in post-earthquake assessment

Prompted by the critical role of post-earthquake inspections, for both emergency response and occupancy, and the need for its fast performance in earthquake damaged areas, several efforts towards facilitating speedier condition assessments have been proposed. These efforts include the creation of evaluation methods based in SHM, Remote Sensing and Computer Vision. These methods attempt to complement current manual practices by providing a non-subjective and quantitative assessment of the existing structural integrity of critical infrastructure and/or buildings. Overall, sensor networks (SHM) are installed in a very small percentage of existing structures in earthquake prone areas and rarely in the most susceptible infrastructures such as older RC frame buildings. Thus, it is evident that despite the fact that structural sensor data can accurately reflect the state of a building, the slow adoption and high associated cost significantly hinder their practical application for building condition evaluation. Remote sensing methods are advantageous in comparison to other methods in that they are low-risk and offer a rapid overview evaluation of the damage in a large geographic region (Adams, 2004). However, the technology is expensive

and remains developed only so far as to obtain an overview of the damage. Since remote sensing methods involve aerial information retrieval, details regarding the existing structural state of individual buildings are not yet possible by way of remote sensing technology. The application of computer vision to building condition assessment employs image processing techniques to automatically detect structural elements and further to automatically detect visual indicators of damage on the structural element surfaces and retrieve properties concerning the detected damage. Methods in computer vision employ low-cost cameras and image processing methods which are near-real-time, and therefore, are the optimal application for research efforts in post-earthquake assessment procedures.

In order to effectively provide a building condition assessment and quantify damage to a structural element using computer vision, there are two necessary steps. First, the damage to the element must be located in the image (detection). Then, beyond the detection of the existence and location of damaged pixels in the image, the extent of the damage should be identified in a quantitative manner (property retrieval). Several efforts have been made towards both the detection and property retrieval of various types of damage. Those efforts relevant to the work presented in this paper fall into three damage types – cracks, corrosion and spalling – each of which will be discussed in the further sections.

2.2.1 Crack detection and property retrieval

Many machine vision-based methods have been created to automatically detect the presence of cracks on concrete and asphalt surfaces using such techniques as Support Vector Machines (Liu et al., 2002) and Principal Component Analysis (Abdel-Qader et al., 2006). In addition, machine vision-based methods have been created which can also define the location of the crack points within the image such as that proposed by Cheng et al. (2003) using interpolation thresholding and the region growing-based operation proposed by Yamaguchi and Hashimoto (2010). Although crack detection has been thoroughly studied, the same is not true for crack property retrieval which is entirely essential in order to infer meaning from the observed damage. There have been efforts in the field of machine vision to retrieve crack length, thickness and orientation information. Chae et al. (2003) employed an artificial neural network to retrieve crack properties in sewer pipeline images using a well-developed digital scanner. However, the effectiveness of the network as well as the method for formulating the input is unclear (German et al., 2012). Another method for detecting cracks on the surface of sewer walls was proposed by Yu et al. (2007). This method used a mobile robot system and graph searching technique to calculate the length, width and orientation of the cracks. The drawback of this method is that the start and end points for each crack segment must be manually identified and the robot was required to maintain the same distance from the wall at all times. Zhu et al. (2011) proposed a method to automatically retrieve relative crack properties from the surface of RC structural elements. The method is based first on the

crack detection procedure developed by Yamaguchi and Hashimoto (2010) using edge detection algorithms to speed the search procedures. Then, a binary image thinning algorithm and a distance transform are used to depict the topological skeleton of the individual crack pieces. The distance field for each crack segment was retrieved and related to the orientation and properties of the structural element in order to determine the relative length, width and orientation of each segment. In this method, the relative properties (length, width and orientation) of crack segments can be automatically retrieved in relation to the length and width of the column with less than 2.5% error.
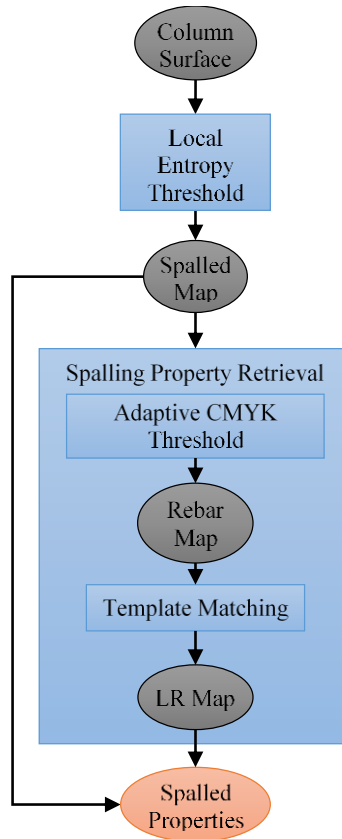

Figure 1 Overview of method in spalled detection and property retrieval (German et al., 2012)

2.2.2 Spalling detection and property retrieval

Although the areas of machine vision-based detection and property retrieval have been studied to a significant extent for both cracks and corrosion, spalling detection and property retrieval has not been studied to the same degree. In post-earthquake evaluations, cracking and spalling are considered significant indicators of the existing health and safety of columns in RC frame buildings. Thus, methods in the automated detection and property retrieval of concrete spalling should be created so that

the existing state of the element and structure can be automatically quantified. The authors have recently published a machine vision-based method in automated detection and property retrieval of spalling on RC column surfaces (Figure 1 (German et al., 2012)). In this method, a local entropy-based thresholding algorithm is employed initially followed by morphological operations (opening/closing/hole-filling) to determine the spalled map. The spalled map is specified as the region of interest (ROI) for further operations executed within the image, and in this method, the ROI includes not only any large spalled regions where reinforcement may be exposed, but also the exposed reinforcement and any visible cracks on the surface of the RC element. At this point, a global adaptive thresholding algorithm is applied throughout the ROI of each channel in the CMYK converted image. Finally, a template matching procedure and a set of morphological operations are used to determine the extent of longitudinal reinforcement which is exposed. In addition, the relative length of the spalled region along the column is determined. Although the method is successful at determining these two values, in order to properly quantify the extent of damage, further properties of the spalled region should be retrieved. The remainder of this paper outlines the overall procedure created by the authors of detecting spalled regions and key relative properties of the spalled region.

3 PROBLEM STATEMENT

In order to automate the visual inspection of buildings, several methods have been proposed. As previously mentioned, spalling is a significant indicator of the current state of the damage to RC columns, and thus, recognizing spalled concrete regions and quantifying the properties of those spalled regions is essential in the post-earthquake assessment of RC columns. Currently, a method does exist which is capable of quantifying spalled regions in terms of two broad classes, however, no method exists for the comprehensive retrieval of the properties of spalled regions on concrete surfaces. The objective of this paper is to present a novel machine vision-based method for the comprehensive detection and property retrieval of spalled regions on RC column surfaces.
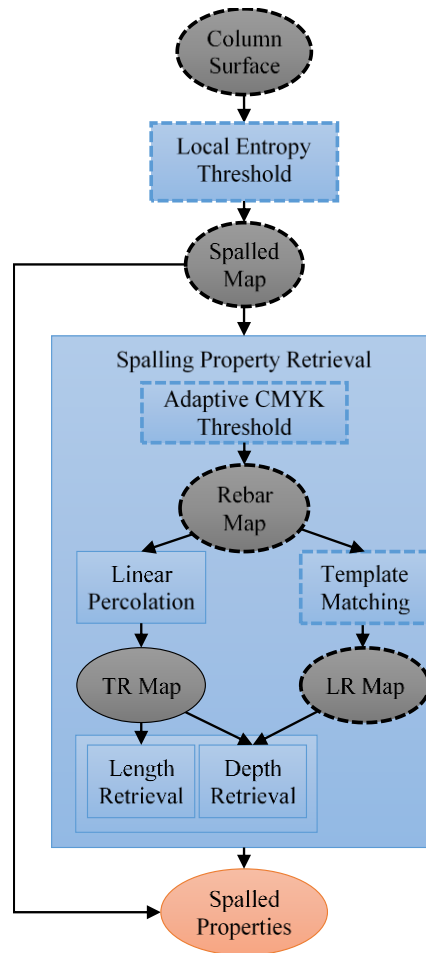
Figure 2 Overview of method in automated spalling detection and property retrieval (where shapes with dashed outlines are those which were also discussed in the authors' previous work)

4 PROPOSED METHOD

The method created by the authors involves the detection of three significant elements: (1) the spalled region; (2) exposed transverse reinforcement; and (3) exposed longitudinal reinforcement. In the method (Figure 2), the spalled region, if any is first detected using the local entropy-based segmentation algorithm developed by the authors (German et al., 2012). The extent of the spalling into the column is calculated primarily based on the amount and type (transverse or longitudinal) of reinforcement exposed. The regions of reinforcement are detected using a threshold in the CMYK color-space (German et al., 2012). Then, the exposed longitudinal reinforcement is detected using a template matching algorithm developed by the authors

(German et al., 2012), and the exposed transverse reinforcement is detected using a state-of-the-art region growing technique which was adapted from a crack detection algorithm. In addition, a binary image thinning algorithm and distance transform are applied to the reinforcement maps in order to retrieve specific properties pertaining to individual exposed bars or segments of bars.
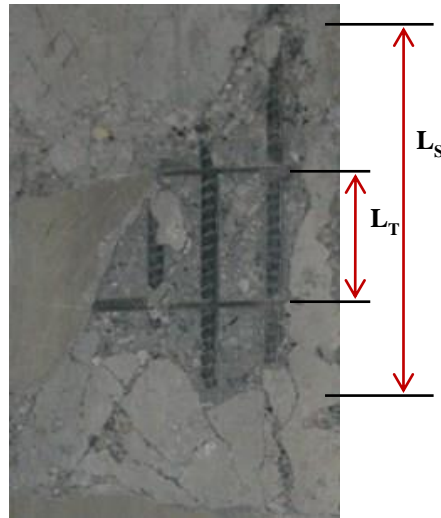
Figure 3 Specification for spalled length classifications (German et al., 2012)

Once the spalled map is detected (according to the method presented in this paper (German et al., 2012)), both the length and the depth (into the column) of the spalled region should be evaluated in order to quantify the extent of spalling on the column. For this work, depth of spalling is classified with respect to the following five categories: (1) no spalling; (2) spalling of concrete cover which does not expose reinforcement; (3) spalling which exposes transverse reinforcement; (4) spalling which exposes longitudinal reinforcement; and (5) spalling which exposes both transverse and longitudinal reinforcement. The length of spalling along the column is depicted by the relative length of the extent of spalling along the vertical (longitudinal) direction of the column L_S, as well as the length between extreme exposed transverse reinforcement bars, L_T (Figure 3).

4.1 Reinforcement detection

Considering the visual appearance of reinforcement, three main distinctive visual characteristics have been identified: (1) ribbed texture along the surface of the potentially exposed reinforcement; (2) the distinct color of steel; and (3) the width of the

longitudinal/transverse reinforcing steel should be significantly less than the width/height of the column. Due to the distinction in the CMYK color-space between the reinforcement pixels and the background/concrete pixels, image segmentation by way of thresholding is an appropriate means of processing the image data.

Once the map representing any indication of exposed transverse and longitudinal reinforcement is produced, the types of reinforcement should be made distinct. In images and video data, due to the larger size of longitudinal reinforcing bars in RC columns, the texture is more prevalent on longitudinal reinforcement. However, the texture is not an adequate visual indicator for transverse reinforcement since the ribs are hard to recognize in medium-to-high resolution images. Therefore, the methods in longitudinal and transverse reinforcement detection differ.

4.1.1 Longitudinal reinforcement detection

In order to properly consider the discernible texture of longitudinal reinforcement, the method in longitudinal reinforcement detection employs the OpenCV template-matching algorithm in each of the four thresholded results (excluding the combination thresholded image) (OpenCV, 2010). The method in longitudinal reinforcement detection is discussed in greater detail in the authors' previous paper which outlines the initial efforts of spalling detection and property retrieval (German et al., 2012).

4.1.2 Transverse reinforcement detection

Since the texture of transverse reinforcement is not as distinct, the method in transverse reinforcement detection considers only the shape and color attributes of the reinforcement detection considers only the shape and color attributes of the reinforcement within the context of a concrete column. The method in transverse reinforcement detection is an adapted version of the percolation-based method proposed by Yamaguchi and Hashimoto (2010). First, the Canny operator is applied to the image to find the pixels with highest gradient magnitude. In addition, the CMYK image is blurred using a 7x7 Gaussian blur. This softens the effect of any texture that is visible, such that the percolation process is more effective.

Table 2
Spalled depth classification (German et al., 2013)

Category	Description	Measure(s)
S0	No spalling	--
S1	Spalling of cover concrete, exposing no reinforcement	L_S
S2	Spalling exposing transverse reinforcement	L_S, L_T
S3	Spalling exposing longitudinal reinforcement	L_S
S4	Spalling exposing both transverse and longitudinal reinforcement	L_S, L_T

Once the edge points are retrieved, the percolation detection is initiated at each pixel location (designated in the edge image) in each channel of the smoothed CMYK image. Based on this method, the process is the following: (1) an edge pixel is selected to initiate the percolation process; (2) this pixel is added to the region, D_P; (3) the neighboring image pixels of those pixels in D_P are added to the region, D_C; (4) all image pixels in D_C which have image intensity (C, M, Y or K value) less than that of the original pixel (the maximum C, M, Y or K value) in D_P are added to D_P; and (5) return to (3) for each pixel added in (4). This process continues until no more pixels can be found with lower image intensity than those in D_P. At this point, the circularity, F_C of D_P is calculated (Equation 1), where C_{count} is the number of pixels in D_P and C_{max} is the maximum dimension of the rectangle bounding D_P. This measure is an indication of the shape of the detected region of pixels. As F_C approaches zero, the shape of the region tends toward linear. Conversely, as F_C approaches one, the shape of the region tends towards circular. Thus, for the detection of transverse reinforcement, regions with a circularity measure less than 0.18 and an approximate angle between -20° and +20°, all of the pixels in D_P are marked as transverse reinforcement pixels.

$$F_c = \frac{4 \times C_{count}}{\pi \times C_{max}^2} \qquad \text{(Eq. 1)}$$

Once this process is completed for each channel, the results for the individual channel percolations are combined using a simple *OR* operation, such that if a pixel is detected as transverse reinforcement in any of the channel percolation procedures, it is also defined as transverse reinforcement must be isolated in order to retrieve the value, L_T. In order to do this, a binary image thinning algorithm (Cychosz, 1994) is used in combination with a Euclidean distance transform (Fabbri et al., 2008) is employed in the same manner as the crack property retrieval work discussed in this paper (Zhu et al., 2011). In addition, this procedure serves to remove pixels which may be false negatives (falsely detected transverse reinforcement pixels).

4.2 Quantification of spalled properties

Once the spalled region and any amount of exposed transverse and longitudinal reinforcement have been detected, the extent of spalling on the RC column should be quantified. The measure of how extensive the spalling is into the column (depth) is calculated by way of a classification stage. The column is dispensed into one of the five categories presented at the beginning of this section and further explained in Table 2. This table also displays the measure(s) which help to classify the extent of spalling along the length of the column that can be retrieved in each category.

Table 3
Results for automated method in spalled depth classification

		Manually Classified				
		S0	S1	S2	S3	S4
Automatically Classified	S0	11	0	0	1	0
	S1	1	8	0	0	0
	S2	0	1	1	0	0
	S3	0	1	0	5	10
	S4	0	3	1	4	32
Accuracy		97.53%	93.18%	97.22%	70.97%	77.55%

In order to measure the extent of spalling along the longitudinal axis of the column (length) the two dimensions, L_S and L_T, are calculated. The length of the spalled region, L_S can be determined directly from the spalled map result at the summation of the spalling detection stage. As previously mentioned, the map represents the location of each spalled pixel in the image or video frame. A novel connected component labeling algorithm is then applied to these regions in order to find the pixel measurement for L_S. The connected component labeling algorithm shifts through every pixel in the image grouping each set of "detected" pixels which border one another into distinct regions. Connection is based on 8-connected objects, and the result is an integer matrix representation of the spalled map with each element index corresponding to the pixel location in the image and value equal to the distinct region number. From this information, the region with the largest area (greatest number of pixels) is determined, and this region is considered as the spalled area of interest for this length measurement. A bounding box oriented in the same direction as the detected column is then created surrounding this region, and the length of this bounding box in the direction parallel to the column's longitudinal axis is considered the pixel representation of L_S measurement. The relative measurement for the spalled length is also calculated with respect to the pixel representation of the width of the column. The length between extreme exposed transverse reinforcing bars, L_T is calculated from the segments resulting from the transverse reinforcement detection algorithm. For each segment detected, a bounding box is created around the entire region of pixels. Then, each box/segment is sorted according to the vertical coordinate of the center of the box. Since the image is oriented according to the axes of the detected column, the difference between the vertical coordinates of the first and last segments in the list is the pixel measurement for L_T. The relative measurement for the length between extreme exposed transverse reinforcing bars is also calculated with respect to the pixel representation of the width of the column.

5 IMPLEMENTATION AND RESULTS

5.1 Implementation

A prototype was developed to detect and retrieve the properties of the spalled regions on RC column surfaces using Microsoft Visual .NET, OpenCV and EmguCV (2010). The methodology presented in this paper is implemented and integrated into the prototype which was developed by the Construction Information Technology Laboratory originally at the Georgia Institute of Technology as an independent module. OpenCV is a collection of C functions and C++ classes. Many popular image processing and computer vision algorithms have previously been implemented in these collections. EmguCV is used as a wrapper to enable the OpenCV functions to be used in the Microsoft Visual .NET environment.

5.2 Results

5.2.1 Validation

The prototype was tested by the authors to collect the images/videos of structures that were damaged in the January 2010 Haiti earthquake. A comprehensive database was created for the purpose of this work including this data in addition to various other images of post-earthquake damaged and non-damaged columns (such as those in the NEES earthquake database (2009)). The performance of the method in spalled property retrieval is evaluated using the calculated percent error (Equation 2) and accuracy (Equation3). The performance of the method is measured with respect to the depth classifications and length measurements.

$$\%\,Error = \left(\frac{Actual - Measured}{Actual} \right) \cdot 100 \qquad \text{(Eq. 2)}$$

$$Accuracy = \frac{TP + TN}{TP + FP + FN + TN} \qquad \text{(Eq. 3)}$$

where TP = object pixels correctly detected as object pixels; FN = object pixels wrongly detected as background pixels; TN = background pixels correctly detected as background pixels; and FP = background pixels wrongly detected as object pixels

5.2.2 Spalling property retrieval performance

For the database of 88 images, the overall accuracy for the classification of the depth of spalling on RC column surfaces was calculated as 87.53%. In addition, the accuracies for each individual class were calculated as 97.53% (S0) 93.18% (S1), 97.22% (S2), 70.97% (S3) and 77.55% (S4). Table 3 shows the results of the classification. In this table, the columns represent

the number of sample images which were manually classified in each category and the rows represent the number of sample images which were classified into each category by way of the automated method presented in this paper. Therefore, the sum of the values in each row is equal to the number of images of each class which was analyzed in the test, and the sum of the values in each column is equal to the number of images detected as each class. Finally, this means that the values in the *(i,j)th* cells where $i \neq j$ represent all of the false positive results (those images classified erroneously), and the values in the *(i,j)th* where $i = j$ represent all of the true positive results (those images classified correctly).

The performance of the method in spalled length calculation is determined using Equation 2 where the manually measured distances (L_S and L_T) relative to the actual measured width of the column are compared with those retrieved automatically. For those test images which appear to have some degree of spalling (S1-S4) the average percent of error and the standard deviation in the measurements are displaced in the first column of Table 4. Likewise, for those test images which are designated as having exposed transverse reinforcement, the average percent error and the standard deviation in the measurements regarding this exposed transverse reinforcement are shown in the second column of Table 4. Figure 4 shows the intermediate results for the method in transverse reinforcement detection and property retrieval for a sample image.

Table 4
Measurement error for length retrieval in
88 spalled images

	L_S / b	L_T / b
Average	4.22%	8.05%
Sdv	2.37%	5.74%

*L_S, L_T defined in Figure 3; b = structural
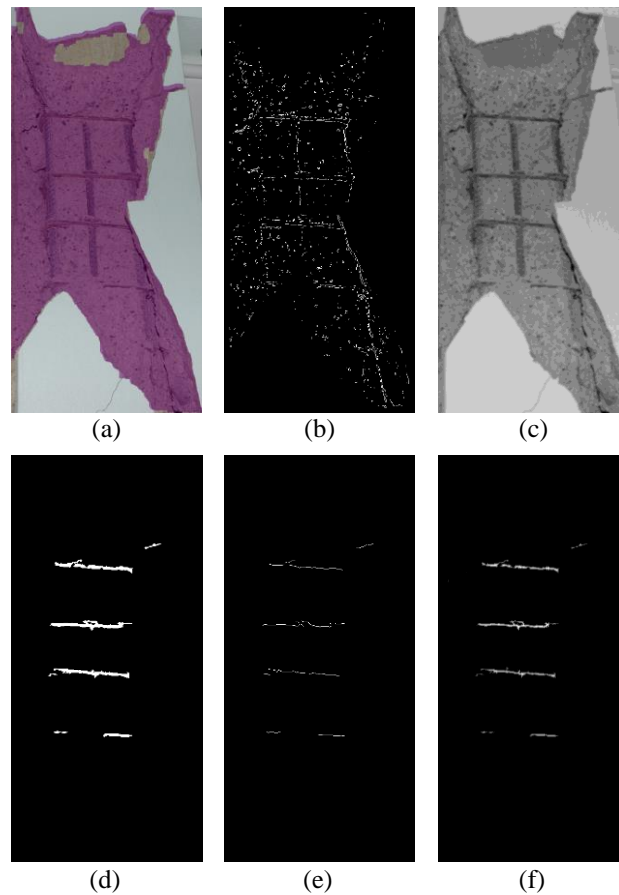element (column) width in pixels

Figure 4 Intermediate results for the method in automated transverse reinforcement detection: (a) spalled map; (b) edge map;

(c) smoothed image (Cyan channel); (d) transverse reinforcement map; (e) skeleton; and (f) distance map

5.3 Analysis of results

It is necessary to evaluate the robustness of the method in spalled property retrieval. Several factors are pertinent to computer vision applications. In this evaluation in particular, the following five factors are considered: (1) blur; (2) illumination; (3) camera shift; (4) occlusion and (5) scale variation. The effects of (2) illumination and (5) scale variation were previously mentioned with respect to an overview of the authors' work in this area. In order to evaluate the robustness of the method to each of these factors, the precision (Equation 4) and recall (Equation 5) were calculated for the resulting image at the first stage of the procedure (e.g., Figure 4 (a)) under varying degrees of distortion as explained in greater detail in the following. The analysis is performed on the spalled map because the output of the overall method is most heavily dependent on the level of sensitivity regarding the detection of the entire spalled region. Further, this evaluation procedure is performed for each image and the averages across each level of distortion for each image are represented in the results (Figure 5).
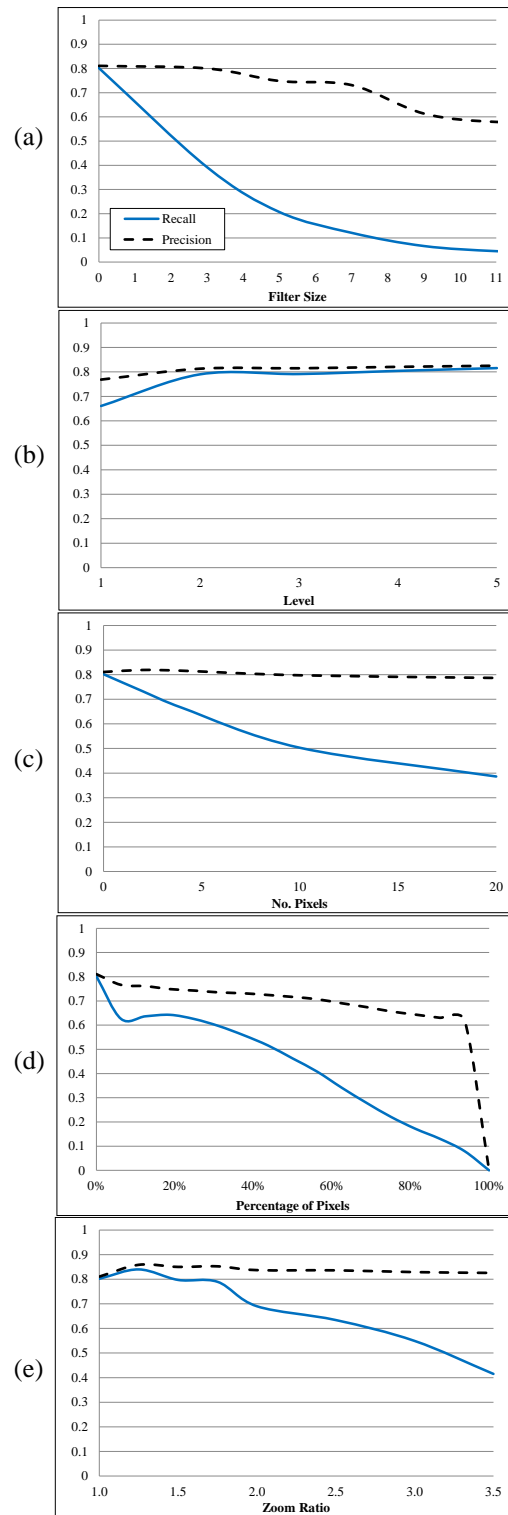
Figure 5 Precision and recall curves for analysis of sensitivity of spalled property retrieval method to: (a) blur; (b) illumination; (c) shift; (d) occlusion; and (e) scale (German et al., 2012)

$$\mathrm{Pr}\mathit{ecision} = \frac{TP}{FP + TP} \qquad\qquad (\text{Eq. 4})$$

$$\mathrm{Re}\mathit{call} = \frac{TP}{TP + FN} \qquad\qquad (\text{Eq. 5})$$

where TP = the number of spalled pixels correctly detected as spalled pixels, FP = the number of background pixels incorrectly detected as spalled pixels and FN = the number of spalled pixels incorrectly detected as background pixels

Blur is oftentimes present in an image or video frame as a result of misplaced focal points. In order to simulate this effect, the original images in the databases are convolved with uniform disk filters of varying radii. The uniform disk filter acts as an averaging mechanism for the pixel neighborhood designated by the filter radius. Then, each of these images are re-evaluated and the comparison across the different degrees of blur is shown in Figure 5(a). Illumination is a metric concerned with the amount and effect of lighting within the image. Depending on the level of illumination, it can be exceedingly difficult to discern key details in an image such as lines, corners, textures, etc. Since lighting is not a controlled variable in the application area of this work, the sensitivity to illumination for the method in automated spalled property retrieval is evaluated. In order to measure the robustness of the method to illumination, five levels of illumination (L1-L5) are imposed on each of the images in the testing database and the precision and recall values of the procedure were re-evaluated. From the curves in Figure 5 (b), it is evident that the method is robust in overly-lit conditions and mildly sensitive in low light scenarios due to the textured nature of the methods in spalling and reinforcement detection. The third metric for evaluating the robustness of the method is blur which has been caused by a physical shift in the camera at the time of image capturing. The physical shift in the camera at the time of image capturing. The physical shift may be the result of a slow shutter speed setting on a still camera or frame-to-frame shifting in video cameras- The effect of shift-blur was manufactured in the original images with a range of linear digital filters at each of the principal orientations (0°, 45°, 90° and 135°). Each of these altered image datasets was evaluated and the trend of the effect of camera shift is displayed in Figure 5 (c). As the amount of shift increases, the recall also decreases revealing that the introduction of a shift due to camera movement increases the false detection ratio. The fourth metric evaluated in this work is occlusion, the partial or full blocking of the desired object of detection by some other object in the image frame. Both horizontal and vertical blocks were artificially introduced across the width and along the length of each image in the database at varying sizes in order to simulate the effects of occlusion. These images were evaluated and the results are shown in Figure 5 (d). It is evident in this figure that the robustness of the image is inversely related to the percent

of the image, or the object of the detection within the image, which is occluded. Any object pixels which are not occluded will be correctly detected; however, those occluded will not be detected. This will be discussed further in the Future Work section. The final metric for evaluating the robustness of the method presented in this paper is scale variation. An object's size can vary from one image or video frame to the next due to different amounts of zoom or distances between the observer and the object. In order to test the sensitivity of this method to variation in scale each image in the database was cropped (from axes with an origin at the center of the original image) according to increasing zoom ratios and the newly formed set of images were evaluated such that the relationship displayed in Figure 5 (e) could be determined. It is apparent that the method discussed in this paper is overall robust, but mildly sensitive, to variation in scale. This is due to the contextual nature of the method.

6 CONCLUSIONS

The occurrence of a natural disaster, such as an earthquake, poses the need for immediate assessment of each building within the affected area both for safety and re-entry of occupants. It is widely accepted that the current procedures for these assessments are overly qualitative, time-consuming and subjective. Thus, an automated alternative to these existing procedures is desired. Many methods have been created in order to detect the damage which the structures have incurred; however, little work has been found in automatically detecting the regions of spalling on the concrete surface or the properties of those regions.

This paper presents the authors' recent work in quantifying the damage on a RC column in terms of the extent of spalling on the column surfaces. In this method, both the length of the spalled region along the column as well as the depth of the region into the column are considered. First, the ROI (the spalled map) is obtained via a novel local-entropy-based threshold algorithm previously developed by the authors (German et al., 2012). Then, an adaptive thresholding algorithm is applied throughout the ROI in each of the four channels in the CMYK image in order to obtain the map of all reinforcement within the image. At this point, the longitudinal reinforcement is detected by way of a template matching algorithm and the transverse reinforcement is detected by way of a region growing operation using the edge images as the starting points. A binary image thinning algorithm and Euclidean distance transform are used to calculate the properties of the detected damage. The method is implemented in a C# based prototype and real damaged concrete column images from the 2010 $M_w = 7.0$ earthquake in Port-au-Prince, Haiti along with various image from post-earthquake damaged buildings were used to validate the work presented

in the paper. The test results indicate that the method in spalled property retrieval is more than adequate and that the depth and length of the spalled region relative to that of the column can be determined with high accuracy.

7 FUTURE WORK

Future work will focus on improvements in the current method in spalled region property retrieval as well as the implementation of this method such that the existing state of a RC column can be determined automatically from video data. The existing method could be further developed in order to classify the depth of spalling according to more specific and applicable ways. The relationship between reduction in strength or stiffness and the visible damage observed on the surface of the RC columns should be studied in greater depth. Most specifically, spalling into the core of the column is significant in the reduction of strength/stiffness of a RC column; this state should be studied and a method should be developed which is capable of classifying a RC column as "spalled into the core" based solely on the visible damage which can be observed. Overall, the authors plan to incorporate the work presented in this paper with that work carried out by the authors concerning crack property retrieval (Zhu et al., 2011) and column detection (Zhu et al., 2010) in order to automatically retrieve an estimate of the existing state of a RC column directly after a disaster based only on the visual damage which can be observed in the video data.

ACKNOWLEDGMENTS

REFERENCES

Abdel-Qader, I., Pashaie-Rad, S., Abudayyeh, O. and Yehia, S. (2006). PCA-Based Algorithm for Unsupervised Bridge Crack Detection, *Advances in Engineering Software, Elsevier, 37* (12): 771-778.

Adams, B.J. (2004). "Improved disaster management through post-earthquake building damage assessment using multi-temporal satellite imagery," In *Proceedings of the ISPRS XXth Congress, Vol. XXXV,* 12-23 July 2004, Istanbul, Turkey.

Aldunate, R., Ochoa, S.F., Peña Mora, F. and Nussbaum, M. (2006). Robust Mobile Ad Hox Space for Collaboration to Support Disaster Relief Efforts Involving Critical Physical Infrastructure. *Journal of Computing in Civil Engineering, ASCE 20* (1): 13-27 (2006).

Applied Technology Council (ATC). (1995). "ATC-20-2, Addendum to the ATC-20 Postearthquake Building Safety Evaluation Procedures," Applied Technology Council. Redwood City, CA.

Chae, M.J., Iseley, T. and Abraham, D.M. (2003). "Computerized Sewer Pipe Condition Assessment," In *Proceedings of the ASCE International Conference on Pipeline Engineering and Construction,* July 13-16. 2003, Baltimore, MD, 477-493.

Chen, P.H. and Chang, P.L. (2006). Effectiveness of neuro-fuzzy recognition approach in evaluating steel bridge paint conditions, *Canadian Journal of Civil Engineering, 33* (2006): 103-108.

Chen, P.H., Yang, Y.C. and Chang, L.M. (2010). Box-and-Ellipse-Based ANFIS for Bridge Coating Assessment, *Journal of Computing in Civil Engineering, ASCE, 24* (5): 389-399.

Chen, P.H., Shen, H.K., Lei, C.Y. and Chang, L.M. (2012). Support-vector-machine-based method for automated steel bridge rust assessment, *Automation in Construction, Elsevier, 23* (2012): 9-19.

Cheng, H., Shi, X. and Glazier, C. (2003). Real-time image thresholding based on sample space reduction and interpolation approach, *Journal of Computing in Civil Engineering, ASCE, 17* (4): 264-272.

Cychosz, J. (1994). "Efficient Binary Image Thinning using Neighbourhood Maps," Academic Press Graphics Gems Series-Graphics Gem IV, ISBN 0-12-336155-9, 465-473.

Fabbri, R., Costa, L., Torelli, J. and Bruno, O. (2008). 2D Euclidean distance transform algorithms: a comparative survey, *ACM Computing Surveys, Association for Computing Machinery (ACM), 40* (1), 2:1-2:44.

Federal Emergency Management Agency (FEMA). (2008). *Structures Specialist Position Description,* DisasterEngineer.org – US&R Structures Specialist Resource. Available online: http://www.disasterengineer.org/LinkClick.aspx?fileticket=7LaKP4hU0jU%3d&tabid=57&mid=397 (Sept, 2012).

Federal Emergency Management Agency (FEMA) (2006), "National Urban Search and Rescue Response System – Structure Specialist Position Description", last visit: http://www.disasterengineer.org/library/Struct%20Spec%20PD%20July%202006.pdf (Dec. 2008).

Federal Emergency Management Agency (FEMA). (2009). *Module 1C Structural Engineering Systems – Part 3,* Retrieved from Federal Emergency Management Agency.

German, S., Jeon, J., Zhu, Z., Bearman, C., Brilakis, I., DesRoches, R. and Lowes, L. (2013). Machine Vision-Enhanced Postearthquake Inspection, *Journal of Computing in Civil Engineering, ASCE, 27* (6): 622-634.

German, S., Brilakis, I. and DesRoches, R. (2012). Rapid Entropy-Based Detection and Properties Measurement of Concrete Spalling with Machine Vision for Post-Earthquake Safety Assessments, *Advanced Engineering Informatics, Elsevier, 26* (4): 846-858.

Kostoulas, D., Aldunate, R., Peña Mora, F. and Lakhera, S. (2006). "A Decentralized Trust Model to Reduce Information Unreliability in Complex Disaster Relief Operations," In *Proc. 13th EG-ICE Workshop on Intelligent Computing in Engineering and Architecture,* Ascona, Switzerland, June 25-30, 2006, LNCS 4200, 383-407.

Lee, S., Chang, L.M. and Skibniewski, M. (2006). Automated recognition of surface defects using digital color image processing, *Automation in Construction, Elsevier, 15* (2006): 540-549.

Lee, S. (2010). An eigenvalue-based recognition method and its application to bridge coating, *Innovation in Architecture Engineering and Construction.*

Liu, Z., Shahrel, A., Ohashi, T. and Toshiaki, E. (2002). "Tunnel crack detection and classification system based on image processing," In *Proc. SPIE Vol. 4664, Machine Vision Applications in Industrial Inspection X,* San Diego, CA, USA, 145-152.

McEntire, D.A. and Cope, J. (2004). "Damage Assessment after the Paso Robles (San Simeon, California) Earthquake: Lessons for Emergency Management." Paso Robles.

Network for Earthquake Engineering Simulation (NEES). (2009). NEEShub Databases. Available online: http://nees/org/databases

Open CV. (2010). "Emgu CV: OpenCV in .NET (C"Emgu CV: OpenCV in .NET (C, VB, C++ and More)." Available online: http://www.emgu.com/wiki/index.php/Main_Page (Oct, 2011).

United States Geological Survey (USGS). (2012). "Earthquake Facts and Statistics Graphs," *Earthquake Hazards Program,* Washington, D.C.: U.S. Department of the Interior.

United States Geological Survey (USGS). (2006). "Earthquake Hazards – A National Threat," Washington, D.C.: U.S. Department of the Interior.

United States Fire Administration (USFA). (1994). "Search and Rescue Operations Following the Northridge Earthquake," Los Angeles: Federal Emergency Management Agency.

Yamaguchi, T. and Hashimoto, S. (2010). Fast crack detection method for large-size concrete surface images using percolation-based image processing, *Machine Vision and Applications, Springer, 21* (5): 797-809.

Yu, S., Jang, J. and Han, C. (2007). Auto inspection system using a mobile robot for detecting concrete cracks in a tunnel, *Journal of Computing in Civil Engineering, ASCE, 17* (4): 255-263.

Zhu, Z. and Brilakis, I. (2010). Concrete Column Recognition in Images and Videos, *Journal of Computing in Civil Engineering, ASCE, 24* (6): 478-487.

Zhu, Z., German, S. and Brilakis, I. (2011). Visual Retrieval of Concrete Crack Properties for Automated Post-Earthquake Structural Safety Evaluation, *Journal of Automation in Construction, Elsevier, 20* (7): 874-883.